Interstellar Matter Kinematics in the Magellanic Clouds

by

Charles Weston Danforth

A dissertation submitted to The Johns Hopkins University in conformity with the requirements for the degree of Doctor of Philosophy.

Baltimore, Maryland

April, 2003

Abstract

It is impossible to understand the stars which make up our galaxy without understanding the properties and kinematics of the interstellar medium (ISM). I study the ISM of the Magellanic Clouds using three different, complimentary datasets. The first is a set of 141 far-ultraviolet (FUV) spectra taken by the *Far Ultraviolet Spectroscopic Explorer (FUSE)* satellite of sight lines toward hot, OB stars in the Magellanic Clouds. I use these stars as background sources and study the absorption in the intervening ISM. *FUSE* data contain hundreds of transitions which probe a wide variety of conditions in the ISM from cold, molecular gas to hot, ionized material. Secondly, I use a collection of emission-line images of the Magellanic Clouds in Hα and red continuum light to provide a morphological context for the FUV absorption data. Finally, I present a set of 99 longslit echelle optical emission spectra to act as a bridge between the kinematics seen in the absorption spectra and the morphology seen in the images. These data lack the broad range of ISM diagnostics present in the *FUSE* data, but feature spatial resolution instead. I use the combination of optical images and optical spectra to classify each sight line into a set of morphological categories.

The diagnostic power of this combined dataset is immense. I use these datasets to search for global patterns in the Magellanic ISM. In particular, I measure the velocities, widths, and column depths of the absorption features in five different FUV transitions and two optical transitions. Various other data from the literature is added to this and I search for correlations. The picture that emerges is one of a three-phase ISM with cold, warm, and hot phases. The kinematics and distribution of each phase bear little resemblance to each other.

Additionally, I use the high velocity resolution to perform two more focussed investigations on the global dataset. First, I study the ionization structure along sight lines, a good probe of temperature and radiation properties in the ISM. I find that the different morphological classes of objects exhibit different ionization characteristics and that the LMC and SMC show different ranges of ionization. I undertake a similar project to study dust depletion in the ISM of the Magellanic Clouds. Again, different classes of objects display different characteristic profiles and depletion values.

Finally, I carry out two investigations of specific ISM structures using small subsets of the emission and absorption data. These show how detailed analysis of the data can shed unprecedented light on the structure and properties of the ISM at smaller scales. In the first case, I investigate the interaction between the ISM and the wind of an luminous blue variable and determine that it is moving through the disk of the LMC at a high speed.

In the second case, I use several emission and absorption spectra to probe the properties of a bright H II region in the SMC and the supernova remnant (SNR) which lies in front of it. I determine the three-dimensional geometry of the region, determine key shock parameters of the SNR, and find that the nebular ISM is fairly quiescent. The FUV flux from the many massive stars within the H II region photoionize the material in the SNR and make optical investigation very difficult. I discuss the implications of SNRs in H II regions and what effect this might have on the search for more distant objects.

Thesis Advisor: Dr. William P. Blair

Dissertation Summary

0.1 Introduction to the ISM

When we look up into the night sky, with a very few exceptions, all we see are stars. Yet the properties and distribution of the stars are governed by the underlying structures in the invisible material between them; the interstellar medium (ISM). The stars we see were formed from this gas and some of it will eventually return into the gas once again. The ISM, in turn, is heated, enriched, compressed, and transported from one part of the galaxy to another by the effects of stars. Most of the stars in our Galaxy are like our sun or smaller and have very little effect on the ISM. Rather, the dynamics of the ISM are driven by the hot, massive, luminous stars; the relationship between massive stars and the ISM is a symbiotic cycle.

With a small telescope and a dark sky we can start to see the interaction of these hot stars and the gas and dust that surround them. Reflection and emission nebulae surround young star clusters and form the familiar Pleiades, the Orion Nebula, and so forth. These nebulae are the remnants of stellar nurseries now heated and disrupted by the stars of their own creation. The delicate filaments of supernova remnants (SNRs) like the Cygnus Loop, the Crab Nebula, and the Vela SNR show where a shock wave from a dying massive star has heated and compressed the surrounding gas. The supernovae themselves enrich the gas with heavy elements created at the cores of the stars. Massive Wolf-Rayet (WR) stars throw off the outer layers of their atmospheres into dramatic rings of heated gas. Planetary nebulae like the Dumbbell or Ring are the products of lower-mass stars reaching the end of their lives and throwing off their outer layers into the ISM again.

There is endless variety in the ISM and endless beauty. It is impossible to understand our Galaxy and the stars we see without understanding the interstellar material which surrounds, forms, and results from stars.

0.1.1 An ISM Beastiary

The most common way of observing the ISM is via line emission at optical wavelengths. We see optically emitting gas organized into different kinds of structures. H II regions are characterized by emission from recombining hydrogen. They are usually seen around hot O and B type stars; stars cooler than T$\sim$20,000K (spectral types A and later) don't produce many hydrogen-ionizing photons and thus don't factor into the ionization of the ISM. The size of the ionized region, or 'Stromgren sphere', is a function of the density of the medium and the ionizing flux of the star (Osterbrock 1989). The heated, ionized material within the Stromgren sphere has a higher pressure than the surrounding, cooler material, thus the ionized gas expands until a pressure equilibrium is reached. Stars also produce strong stellar winds (outflows of mass at high velocities) which further heat the surrounding medium. These winds tend to blow bubbles in the cool, dense ambient medium. More massive stars tend to have the most massive and fastest winds and are thus most efficient at interacting with the ISM.

When a massive star reaches the end of its life $10^6 - 10^7$ years after formation, it explodes as supernova (SN). With a supernova explosion comes a violent shockwave as material expands at velocities of thousands of kilometers per second (much higher than the $\sim$10 km s^{-1} interstellar sound speed). When the shock encounters the ISM, low ionization species are accelerated and further ionized to much higher levels. Neutral species are heated through collisions with these shocked ions. Temperatures can reach millions of degrees behind the expanding shock fronts. Cooling time is proportional to n^{-2} (where n is the number density), thus cooling is fairly rapid in dense regions as energy is lost through line radiation.

Isolated SNRs and the H II regions around single stars are typically on a scale of a few to a few tens of pc in size. However, massive stars frequently form in clusters which may include multiple, UV-bright O and B-type stars. These OB associations will produce a correspondingly larger ionized nebula through their combined photoionization. The combined winds and any supernovae which go off in the cluster will create a bubble of hot, ionized gas. Through time and subsequent supernovae, the bubble will expand into a hollow superbubble, which can be up to 100 pc in size.

At the largest scale are the supergiant shells; kiloparsec-scale holes in the cold gas distribution, the largest structures in the ISM. They are distinguished from smaller structures in that they are larger than the scale height of their host galaxy (Grebel 2002). Supershells do not usually show up in optical emission. Rather, they are obvious from radio observations of other galaxies where they appear as kiloparsec-scale voids in the H I distribution (Meaburn 1980; Chu 1996; Kim et al. 1999). They may be relics of past star formation events, infalling extra-galactic clouds (Tenorio-Tagle et al. 1987), or possibly even gamma ray burst remnants (Efremov, Elmegreen, & Hodge 1998; Loeb & Perna 1998).

Away from the bright nebulae lies diffuse ionized gas (DIG). DIG is seen throughout the ISM and is the product of ionizing photons which leak out of porous H II regions and from field OB stars and shocks from SN (Reynolds, Haffner, & Madsen 2002). DIG is characterized by a low-level Hα emission but, in total, can make up a sizeable fraction of the total Hα luminosity of a galaxy (Kennicutt et al. 1995).

0.1.2 Models of the ISM

One of the first theoretical models of the ISM was the two-phase model developed by Field, Goldsmith, & Habing (1969). In the two-phase model, cold clouds with temperatures of T<300 K and densities of a few tens of particles per cubic centimeter exist in pressure equilibrium with a warm (T$\sim$10^4 K), diffuse (n$\sim$0.1 cm^{-3}) phase. The majority of the mass is in the cold phase while the majority of the volume is occupied by the warm phase. Heating of the warm phase is

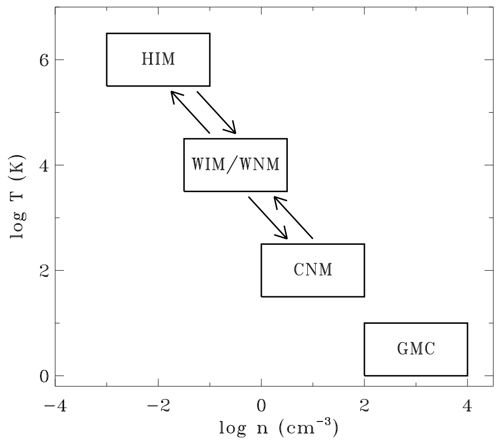

Figure 0.1 — The three-phase model of the ISM (after Ikeuchi 1998).

accomplished through X-ray and ultraviolet (UV) radiation and low-energy cosmic rays. However, sufficient heating sources have never been found to match the observed temperatures in the warm ISM (McCray & Snow 1979).

In the mid-1970s, a three-phase ISM model was developed. Early X-ray observations and the discovery of far ultraviolet (FUV) O VI absorption suggested a hot, coronal gas phase near 10^6 K. Cox & Smith (1974) suggested that a realistic supernova rate was sufficient to create the observed coronal gas and that interacting supernova remnants could hollow out tunnels of hot material through the warm and cold gas. McKee & Ostriker (1977) expanded this theory and suggested that the volume fraction of the hot gas is much larger than that of the warm or cold gas. Rather than tunnels of hot gas through a cooler medium, the cool gas exists as clumps and isolated clouds in a surrounding hot environment. Shocks from supernovae travel easily through the diffuse hot gas and keep the temperatures high. Since hot, diffuse gas does not cool easily, it can exist at nearly the same temperature for long after the supernova shocks had dissipated.

The modern view of the ISM is based largely on the three-phase model of McKee & Ostriker illustrated schematically in Figure 0.1. The ISM is populated by the cold neutral medium (CNM), hot ionized medium (HIM) energized by SNRs, and warm gas with ionized and neutral components (WIM and WNM). The warm phase is maintained through photoionization by hot stars (Reynolds, Haffner, & Madsen 2002) and make up the observed H II regions and DIG. The three phases are more-or-less in pressure equilibrium with one another. Most of the mass of the ISM is in the form of cold gas while the largest volume is filled with HIM. The precise filling fractions and mass fractions are a matter of some debate and are reviewed by McKee (1990). The phases exchange material through evaporation and condensation at the edges of the coronal gas and by photoionization and line cooling processes.

Very cold (T$\sim$10 K), very dense molecular gas in the cores of giant molecular clouds

(GMCs) represents a fourth phase of the ISM. GMCs have masses of 10^4 $M_\odot$ and higher (sometimes considerably higher) and thus are self-gravitating. Since they are self-gravitating, they are not necessarily in pressure equilibrium with the other three phases (McKee 1990). It is from these clouds that stars form.

On the galactic scale, the distribution of the different phases is related to their kinematics. The coldest gas occupies a thin disk at the galactic mid-plane while the hotter gasses are seen in increasingly inflated distributions. The disk-averaged distribution is modeled exponentially with each phase having a characteristic scale height. Observations are consistent with a scale height for cold molecular and atomic gas of about 70 pc in the Milky Way while the WNM scale height is 260–400 pc. The vertical extents of the WIM and HIM are substantially more uncertain; $\sim$900 pc and 1.6–5 kpc, respectively (see Savage 1995, and sources therein). This warm and hot gas forms the Galactic Halo which surrounds the denser disk gas of the Milky Way. Very recently, using data from the *FUSE* satellite, Sembach et al. (2003) have inferred the presence of an even more tenuous and extended hot corona around the Milky Way that extends for tens of kiloparsecs from the disk.

A major refinement to the three-phase model was proposed in the late 1980s by Ikeuchi (1987) and Norman & Ikeuchi (1989). Previous models used uniformly distributed supernovae to power the HIM phase, but most SN precursor stars are clustered in OB associations along the spiral arms in the disk. Clustered supernovae could create hot bubbles which would exceed the scale-height of the warm and cool gas in the galaxy. This "galactic chimney" effect would efficiently pump hot gas into the halo and explain the large holes empty of H I seen in external galaxies.

0.2 The Magellanic Clouds

The Magellanic Clouds are an ideal laboratory in which to study the ISM. They are a pair of satellite galaxies of the Milky Way located in the southern sky. The Large Magellanic Cloud (LMC) is both closer and physically larger than the Small Magellanic Cloud (SMC). A great many studies have been undertaken to determine the precise distance to each of the Clouds. Throughout this work I assume an LMC distance of 50 kpc and an SMC distance of 60 kpc which are typical of the literature values. The LMC has a mass of 5.3×10^9 $M_\odot$ (Alves & Nelson 2000) or about 2% that of the Galaxy while the SMC has a mass of 2×10^9 $M_\odot$ (Westerlund 1997) or about 1% that of the Milky Way. Together they are by far the largest satellite galaxies of the Milky Way and exist in a class unique between the giant galaxies of the Local Group (the Milky Way, M31, and M33) and the dozens of tiny dwarf galaxies (Mateo 1998). Aside from the dramatic mass and size differences, the Clouds have lower metallicity and higher star formation rates than the Galaxy.

The two Clouds are connected by a 'Bridge' of H I gas and a trail of similar gas—the Magellanic Stream—extends more than half way across the sky as shown in Figure 0.2. The Stream is probably gas stripped from the SMC as the Clouds orbit the Milky Way (Putman et al. 1998, 2003; Brüns, Kerp, & Staveley-Smith 2000). Both galaxies have passed through the plane of the Milky

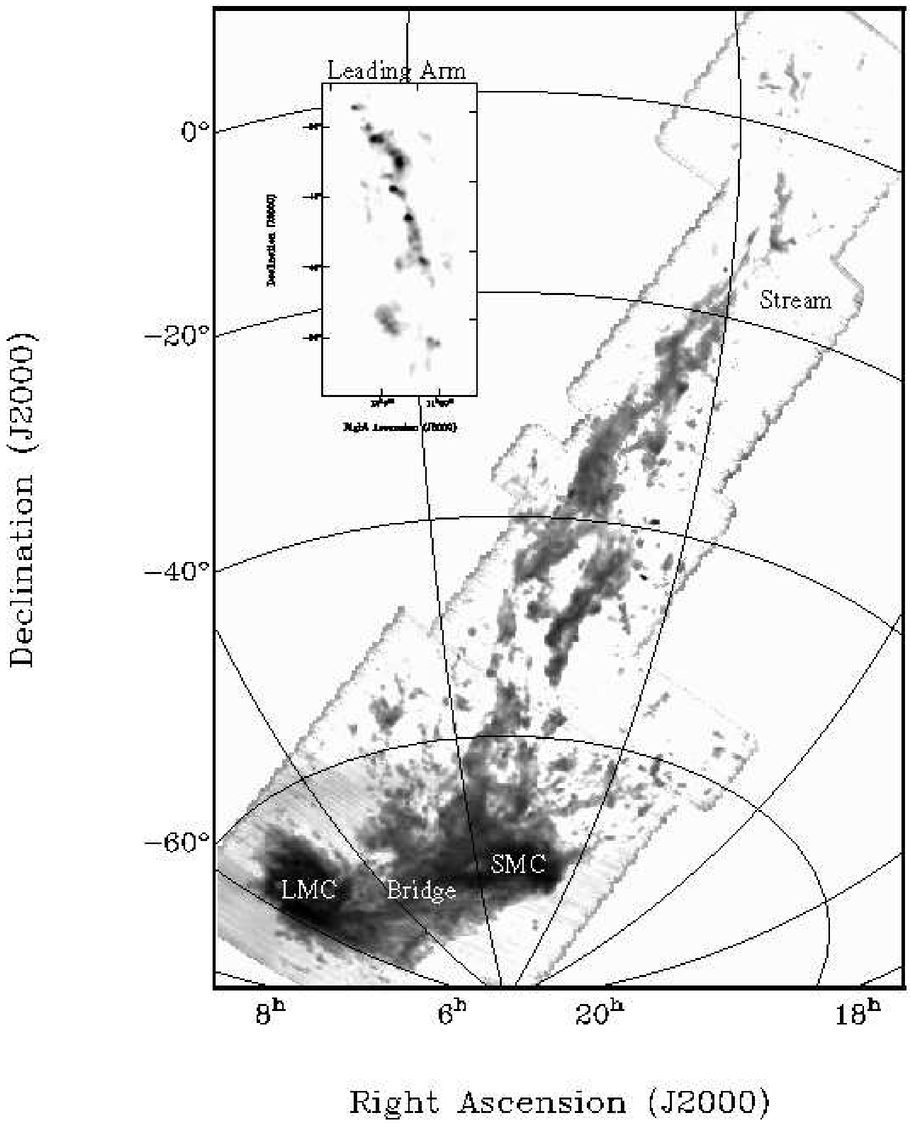

Figure 0.2 — An H I column density map of the Magellanic System from Brüns, Kerp, & Staveley-Smith (2000). Visible in this image are the LMC and SMC at the lower left. They are joined by the Magellanic Bridge. The Magellanic Stream heads northwest from the SMC and shows the orbit of the Clouds around the Galaxy. The Leading Arm, shown as an inset, extends a short distance from the LMC forward along the direction of the orbit.

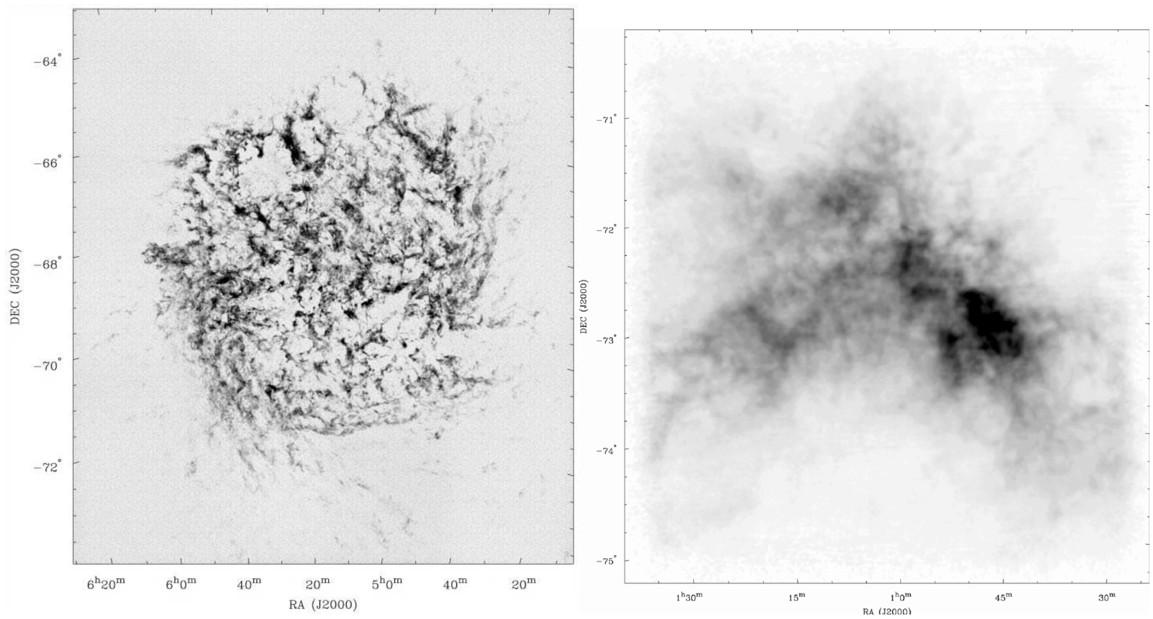

Figure 0.3 — H I images of the LMC, from Kim et al. (1998a), and the SMC, from Stanimirović et al. (1999). Note the floculent spiral arms and general disk morphology of the LMC. The SMC has a more amorphous shape consisting of the bright bar and the eastern wing.

Way multiple times since their formation—events which caused great turmoil in the smaller galaxies and prompted eras of star formation. There is some evidence that the LMC and SMC collided 2×10^8 years ago. This may account for many features of their structure and dynamics (Westerlund 1990).

The overall structure of the LMC is a nearly face-on disk as seen in 21 cm H I maps (Figure 0.3a) with flocculent spiral arms (Kim et al. 1998a). Inclination estimates of the LMC disk vary from 22° to 45° depending on which distance indicators are used (Weinberg & Nikolaev 2001; van der Marel & Cioni 2001). Many holes are seen in the H I distribution from a few parsecs to kiloparsecs in size corresponding, in many cases, to ISM features such as supergiant shells and bubbles. In visible light (Figure 0.4a), the stars are concentrated in a $1°\times4°$ bar similar to those seen in many galaxies including our own, but this bar is notably off-center from the gas disk and may not even be coplanar. The Hα distribution (Figure 0.4b) shows little evidence of the stellar bar and is more reminiscent of the H I disk morphology.

The SMC is smaller and more irregular than the LMC and its morphology is amorphous at both radio and optical wavelengths as shown in Figure 0.3b and 0.5. The three-dimensional structure of the SMC is the subject of continuing debate though it is generally agreed that it is not a disk and covers a relatively large distance along our line of sight (Crowl et al. 2001). A bright 'Bar' runs northeast-southwest and houses most of the mass of both stars and gas. The fainter 'Wing' stretches away to the southeast and connects to the Magellanic Bridge.

One of the most striking features of the Clouds is their wealth of star-forming activity

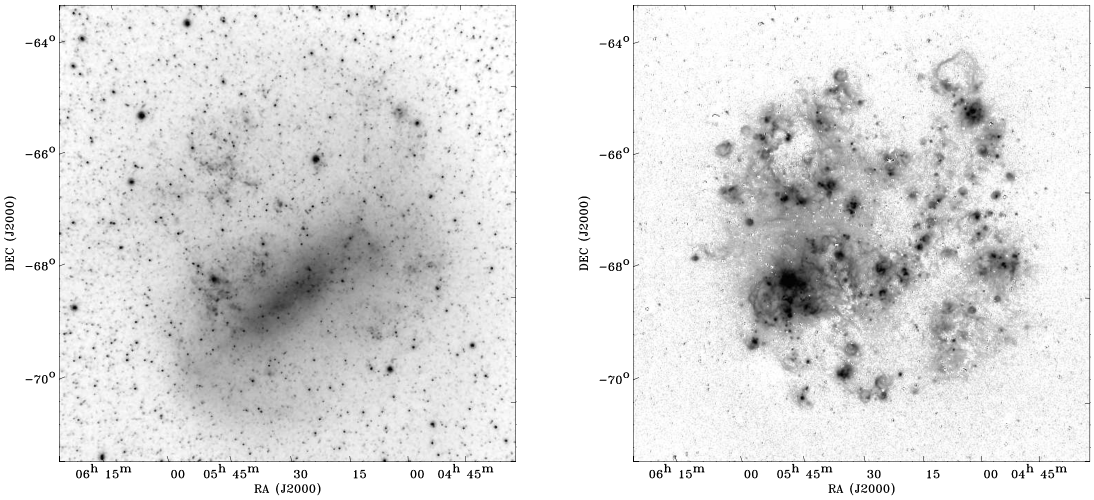

Figure 0.4 — a) The LMC in red continuum light showing the prominent stellar bar. b) A continuum-subtracted Hα image. Both images courtesy of Gaustad et al. (2001).

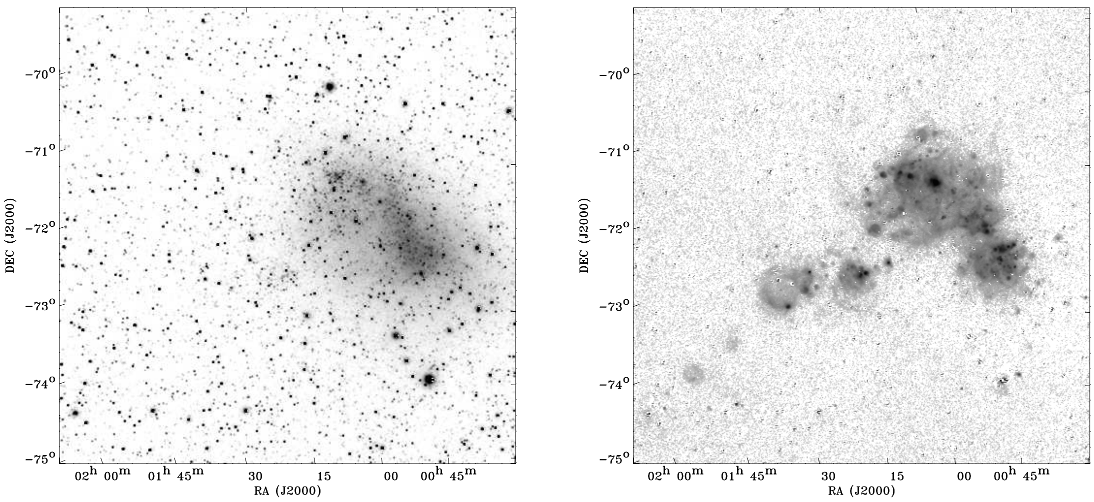

Figure 0.5 — Same as Figure 0.4 but for the SMC.

and the associated rich ISM features as seen in Figures 0.4b and 0.5b. There are hundreds of H II regions, supernova remnants, superbubbles and areas of diffuse emission. Twenty three supergiant shells are seen in the LMC from 600 to 1400 pc (Meaburn 1980; Oey 1998; Kim et al. 1999) and six are in the SMC (Stanimirović et al. 1999). Each Cloud has hundreds of H II regions of all sizes and are rich in diffuse emission.

While the Magellanic Clouds themselves are substantially different in morphology, metallicity, star-formation history, and many other parameters, many of the smaller scale features found in the Magellanic Clouds have direct analogues in our own Galaxy. For many categories of objects, the available Magellanic Cloud samples are larger and easier to study systematically than the Galactic samples, which may be obscured in the disk, at unknown distances, or beset by line-of-sight confusion. With the sensitivity of modern instruments, even individual stars of types rarely observable in our own Galaxy—Wolf-Rayet stars, luminous blue variable (LBV) stars, etc.—are readily detectable in the relatively unreddened Magellanic Clouds. The SNRs N132D and 0540−69.3 in the LMC and E0102−7219 in the SMC share similar morphology with, respectively, the Cygnus Loop, the Crab Nebula and Cas A in the Milky Way. Larger structures such as superbubbles and supergiant shells (Meaburn 1980; Staveley-Smith et al. 1997; Kim et al. 1999) are also obvious in the Clouds. These features are likely similar to Milky Way structures such as the Scutum supershell (Callaway et al. 2000), the W4 Chimney (Reynolds, Sterling, & Haffner 2001), and the Aquila supershell (Maciejewski et al. 1996).

0.3 Scientific Objectives

The Magellanic Clouds are a nearly ideal laboratory for ISM astronomy and are, in many ways, less complicated than our own Galaxy. They also serve as a kind of Rosetta Stone for comparing objects in our own Galaxy with those in more distant ones.

For detailed understanding of galaxies and galactic evolution, we need to understand the distribution and kinematics of the interstellar medium. The optical wavelengths are by far the easiest for astronomers to access, and thus the majority of existing astronomical data and instruments sample visible light. However, the kinematics of the ISM are best studied with a multiwavelength approach; the far-UV, radio, infrared, and X-ray bands contain valuable and unique information to add to the picture.

In this thesis I study the morphology and dynamics of the ISM in the Magellanic Clouds through optical and FUV wavelengths. Optical emission lines tend to probe only a certain temperature regime. The FUV spectral range gives access to a wide range of ISM conditions from H_2 (cold neutral gas) to various singly-ionized ions (warm neutral gas) to O VI (hot ionized gas). In particular, I investigate the correlation between what is seen in the optical and the corresponding FUV structure.

In addition, I am interested in the kinematics of different classes of objects found in the ISM and whether these properties change between the LMC and the SMC. For instance, do all Magellanic H II regions have similar structure and kinematics or do all of them show unique properties? What do the ionization structure and dust-to-gas diagnostics say about the different regions? Do differences in metallicity between the two galaxies show up as differences in the FUV spectral properties?

Finally, I investigate the structure and dynamics of various individual ISM objects within the Magellanic ISM. These objects are likely to be similar to structures in our own Galaxy but are uncomplicated by high extinction, line-of-sight confusion, and distance (hence physical scale) uncertainties. This may cast a new light on processes within the Galactic ISM.

0.4 Methods

The overall goal of this work was to correlate the optical and far-UV morphology and dynamics seen in the ISM of the Magellanic Clouds. To this end, I utilized three different sets of observations.

In Chapter 2, I presented an atlas of 141 *FUSE* observations of sight lines toward early-type stars in the Magellanic Clouds. I also present a set of Hα emission line images showing the optical morphology of the ISM and developing a context for each of the one-dimensional sight lines. In the atlas, I show the absorption structure in nine ionic transitions and six molecular hydrogen transitions for each sight line. These transitions cover a wide range of ISM conditions from cold molecular gas to hot coronal gas. The spectral resolution of *FUSE* provides a velocity resolution of $\sim$15 km s^{-1} and, since the systemic velocities of LMC and SMC are +250 and +150 km s^{-1}, respectively, absorption from Galactic and Magellanic material can be easily differentiated. Furthermore, multiple absorption components in the Clouds can be resolved in many sight lines.

I analyzed the Magellanic absorption data in several ways. First, I determined the profile-weighted mean velocity and line-width of the Magellanic and Galactic absorption components for each sight line in five WNM and WIM ions. During this process, the total apparent column depth was determined as well. Secondly, I modeled the absorption profiles in the same ions with a series of Voigt functions. These models returned velocities, line widths and column depths for each fit component.

Unfortunately, the velocity resolution of *FUSE* is insufficient to fully resolve typical interstellar lines and thus unresolved, saturated structure may exist in some of the data. I present three methods of determining if such saturation exists in an observation.

In Chapter 3, I presented a parallel atlas of 99 ground-based, optical, echelle spectra of the Magellanic Clouds. Many of these observations cover stars also observed by *FUSE* as well as their surrounding nebulosity. In this case, spectral coverage was sacrificed for spatial coverage; a $3\rlap{.}'5$ slit was placed over the target region and shows the velocity structure over a limited spectral range. Hα and the [N II] doublet at $\lambda\lambda$6548,6583 are covered at a resolution equal to that of the FUV absorption data.

Spectral profiles of the emission data were produced by collapsing a $\sim$30$''$ portion of the spectral slit centered on the star or region of interest. These profiles were then fit in the same manner as the absorption data producing profile-averaged mean velocities and widths and component fits.

The spatially resolved echelle data were used along with wide-field Schmidt images to determine the morphology of each *FUSE* and echelle sight line. In many cases, the morphology was evident from the images alone. However, the kinematic information provided by the echelle spectra distinguished expansion structures from quiescent H II regions. The majority of the sight lines were classified into four major morphological categories: field, diffuse H II, H II region, or superbubble.

In Chapter 4, I analyzed the data presented in the two atlases in several ways. Chapters 5 and 6 dealt with the detailed analysis of smaller sub-sets of the data. In the following summary, I review the conclusions drawn from these three chapters of analysis.

0.5 Conclusions

A number of conclusions arise from the analysis in Chapters 4, 5, and 6. While specific conclusions are presented in those chapters, I discuss here the more general conclusions which can be drawn from the thesis as a whole.

0.5.1 Large-scale Patterns

First, it is clear that large-scale, structural patterns in the Magellanic Clouds can be seen in my data. Traditionally, studies of galaxy-wide trends are undertaken with data which samples the entire object rather than a number of one-dimensional sight lines. I use $\sim$90 absorption sight lines to show the rotation sense of the LMC and the results agree well with the better-sampled results from radio H I data (which sample two spatial dimensions as well as velocity space). Similarly, I see results consistent with known studies regarding the three-dimensional structure of the SMC from $\sim$50 absorption sight lines.

In the same vein, I have shown that point-sampled absorption observations can detect the presence of low-column-density material along the sight line which is not related directly to the Magellanic Clouds. Emission-based radio maps provide more thorough sampling but do not necessarily have the same sensitive to low column material.

0.5.2 The Three-Phase Model

Using transitions which sample different temperature regimes reveals an interesting confirmation of the three-phase model of the ISM. Fe II, Si II, P II, and Hα all sample the warm neutral medium. Within a particular sight line, these species tend to show similar component structure at similar velocities. Species which sample other phases of the ISM such as Fe III (WIM) or H_2 (CNM) correlate surprisingly badly with the WNM ions. The WIM, WNM, and CNM phases have distinct kinematics and distributions. This point is further brought home by the qualitative O VI analysis. O VI samples the hot ionized medium and is seen everywhere regardless of Hα morphology. Furthermore, it appears at different velocities than absorption from the cooler material.

0.5.3 Emission and Absorption

It is somewhat difficult to compare emission and absorption data directly. The echelle and *FUSE* data were taken with completely different instruments and special care must be taken to align the data in velocity space. Even the one-dimensional emission profiles (created to compare with the absorption pencil beams) sample a finite spatial distance along the slit. Furthermore, absorption observations only sample data along a finite sight line, to the midpoint of the LMC or SMC typically. Emission data sample material along the entire line of sight. Some of this material undoubtedly lies beyond the OB star serving as a background source for the absorption observation and thus confusion can result.

In some cases, this distinction between finite and infinite sight lines can reveal the three-dimensional geometry of the ISM. Sk $-68°80$ is good examples of this phenomenon. Figure B.34 shows two obvious emission components in Hα, but only one Fe II absorption component. Clearly, the blue-shifted emission represents material which is between us and Sk $-68°80$ while the brighter, red-shifted emission component lies on the far side of the star and is not probed by the absorption data.

With the above caveats in mind, the WNM ion absorption data and the Hα and [N II] emission data agree reasonably well. The LMC rotation curves in P II and Hα are similar in sense if not in the details and there is a correlation between Hα and WNM ionic velocities which does not exist between Hα and either H_2 or Fe III.

0.5.4 Morphology

There are definite trends between different classes of objects. These difference manifest themselves in many ways from depletion and ionization patterns to the emission profiles. For example, most LMC H II regions share a certain range of ionization values and shape of ionization profile. This range and characteristic profile are different from those of LMC field targets and superbubbles.

In some cases, objects classified as one morphology through simple inspection better fit the characteristics of a different class upon detailed analysis. An example of this is the DEM 241 which looks like an H II region in the images but shows superbubble-like ionization and depletion behavior.

Meanwhile the same class of objects in the LMC and SMC can show different behaviors as well. For instance, SMC diffuse H II regions shows much higher ionization than their counterparts in the LMC. This probably reflects differences in the ambient UV field in the two galaxies as well as differences in metallicity.

0.5.5 Detailed Analysis

Finally, I gave two examples of how a detailed comparison between emission and absorption data can be used to explore the kinematics and structure of individual objects in the ISM. The first example, that of the LMC LBV S119, uses a single *FUSE* observation and a single echelle spectrum to determine the three-dimensional geometry of the object and its interaction with the surrounding ISM.

In the second example, I use a larger dataset of six *FUSE* observations and seven echelle spectra to investigate the properties of the large, bright H II region N66 in the SMC. One of these observations showed bright FUV emission from a SNR lying in front of the photoionized nebula. I conclude that the many massive stars nearby are strongly effecting the appearance of the remnant and are making it difficult to detect through traditional optical means. I posit that more SNRs should be seen in OB associations and H II regions and that the use of the far-UV is an effective tool for finding such objects.

0.6 Future Work

There is still considerable science to be done with my three large datasets and this thesis has only scratched the surface. The database of *FUSE* observations is large enough that many H II regions, superbubbles and supergiant shells are sampled by several sight lines and many of these objects have also been observed by multiple echelle slits. The N66 investigation presented in Chapter 6 is a good example of what can be done with multiple FUV and optical echelle spectra.

Roughly a dozen other regions in the Magellanic Clouds feature three or more *FUSE* observations and echelle slits. This list includes the LMC superbubble N206, the SMC H II region N76, the LMC superbubble N119, the cluster of H II regions and SNRs at the southern end of the SMC bar, and more.

The *FUSE* mission is still quite active and is producing more Magellanic Cloud datasets every Cycle. In particular, I am involved in a Cycle 4 program which has scheduled observations of another ~20 Magellanic Cloud sight lines. These observations will provide additional sight lines through objects already observed and presented in this thesis.